processes

MDPI

Article

Permeability Evolution of Naturally Fractured Coal Injected with High-Temperature Nitrogen: Experimental Observations

Shengcheng Wang [1,2,*], Haijian Li [3] and Lanying Huang [1]

[1] School of Civil Engineering, Xuzhou University of Technology, Xuzhou 221018, China; hlymaster@126.com
[2] School of Safety Engineering, China University of Mining and Technology, Xuzhou 221116, China
[3] College of Geology and Mines Engineering, Xinjiang University, Urumqi 830047, China; haijianlee@126.com
* Correspondence: scwang@xzit.edu.cn

Abstract: The permeability of more than 70% of coal seams in China is less than 1 mD, creating difficulties in recovering underground coal methane. Therefore, a new technology of high-temperature nitrogen (HTN_2) injection into the coal seam was proposed to improve the coal permeability and gas extraction rate. In this paper, the effects of the N_2 temperature, injection pressure and cycle number on the permeability of naturally fractured coking coal has been investigated. When HTN_2 was injected into coal samples, the results indicated that the permeability decreased over time in the beginning, suddenly increased to a large value, and was subsequently maintained in a relatively stable range. The maximum permeability ratio increased with the rise of the N_2 temperature and injection pressure. An analysis indicated that the increase of coal permeability was the result of the increase of the global coal strain caused by thermal expansion and the adsorption-induced expansion. The maximum permeability ratios in various cycles of multicycle N_2 injection into the coal sample were all greater than 1.0 while progressively declining. Obviously, the alternating stress was conducive to the further expansion of the coal fractures to increase the coal permeability. However, on the basis of the first period of expansion, re-expansion was difficult and required more energy. The effects of multicycle N_2 injection on coal permeability have been considerably improved when compared with N_2 injection with only one cycle. The research results are helpful for rapidly extracting methane and guaranteeing mine safety.

Keywords: coal permeability; N_2 temperature; N_2 injection pressure; cycle number; triaxial test

Citation: Wang, S.; Li, H.; Huang, L. Permeability Evolution of Naturally Fractured Coal Injected with High-Temperature Nitrogen: Experimental Observations. *Processes* **2021**, *9*, 296. https://doi.org/10.3390/pr9020296

Academic Editors: Zhiqiang Sun, Ge Yi Man and Sheng Yang
Received: 14 December 2020
Accepted: 29 January 2021
Published: 3 February 2021

1. Introduction

Coalbed methane (CBM) is a precious nonrenewable energy [1]. The extraction of CBM can control gas disasters in mines and protect the environment [2]. However, more than 70% of Chinese coal seams' permeability is lower than 1 mD [3], and it is difficult to extract CBM. Plenty of studies on the drainage efficiency improvement of CBM have been conducted [4,5]. Gas injection is one of the main methods for increasing CBM production [6], and CO_2 and N_2 are the most common gases for injection into coal seams. CO_2–Enhanced CBM (CO_2–ECBM) production involves the injection of CO_2 into coal seams to promote the desorption of CBM while simultaneously reducing the output of greenhouse gases into the atmosphere [7,8]. However, CO_2–ECBM can only be used in deep un-mineable coal seams [9]. Zhou et al. found that N_2 injection caused moderate increases in coal permeability [10]. Studies have shown that the coal desorption capacity for CBM increased with an increase of temperature [11–13]. Thus, a new technology of HTN_2 injection into the coal seam has been proposed.

The temperature effect on the desorption and adsorption of CBM has been studied. Li et al. found that the methane permeability increased with the temperature when the effective stress was lower than the thermal stress; otherwise, the methane permeability increased when the temperature decreased [14]. Hu et al. discovered that the N_2 permeability decreased at first, then rose, and finally decreased when the coal temperature was within

100 °C. 50 °C and 80 °C were the lowest and the highest temperature, respectively [15]. Zhao et al. found that the N_2 permeability changed during the heating process; it increased rapidly with the temperature when the percolation threshold value of the coal mass was smaller than the overall porosity [16]. Perera et al. found that the effect of the temperature on the N_2 permeability was not obvious [17]. Zhu et al. found that the thermal expansion and sorption-induced swelling caused by temperature change could affect coal permeability significantly [18]. Peng et al. found that when the diffusivity was low, the change of coal permeability with time displayed a "V" shape. Existing studies mainly focus on the effects of normal temperature N_2 injection or coal temperature on permeability, and the question of how coal permeability changes under N_2 injections with different temperatures and pressures into coal is still not studied [19].

In this study, the effects of the gas temperature, pressure and cycle number on the permeability of naturally fractured coking coal with HTN_2 injections were investigated. A testing system for HTN_2 injections was developed. We tested six specimens from the Pingdingshan Coalfield in China.

2. Experimental Methodology

2.1. Testing System

A testing system for HTN_2 injection for permeability tests was established, as shown in Figure 1. The system can continuously monitor the temperature and pressure of the HTN_2 injection, the axial stress and the lateral stress, and the deformation displacement of the coal sample, etc. During the experiment, a mass flowmeter was used to measure the flow rate at the outlet.

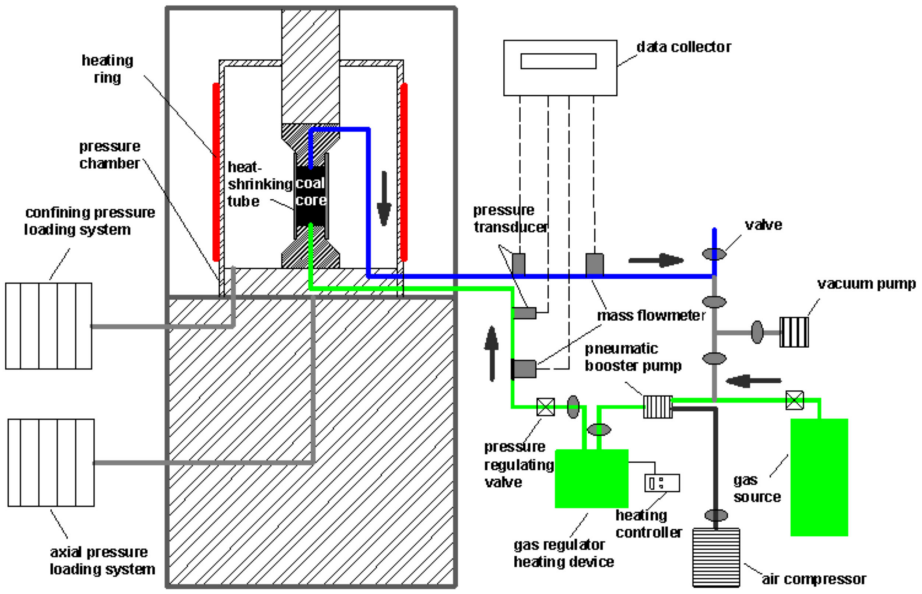

Figure 1. Schematic of the testing system.

2.2. Sample Preparation

The naturally fractured coking coal samples used in the test were taken from the #J15 coal seam of the Pingdingshan Coalfield in China. The physical properties of the coal are shown in Table 1. The large coal blocks were cored, cut and grinded, after which samples with a diameter of 50 mm and a length of 100 mm were obtained. Some of the natural fractures in a typical coal sample are shown in Figure 2a, and fractures distribution of the coal sample after HTN_2 injection are shown in Figure 2b.

Table 1. Physical properties of the Pingdingshan Coalfield coking coal used for testing.

Property	Value
Vitrinite reflection (%)	1.34–2.11
Moisture content (%)	0.95–2.24
Ash yield (%)	10.22–14.03
Volatile matter (%)	20.8–23.5
Fixed carbon (%)	64.2–69.6
Coal density (g/cm^3)	1.45–1.52

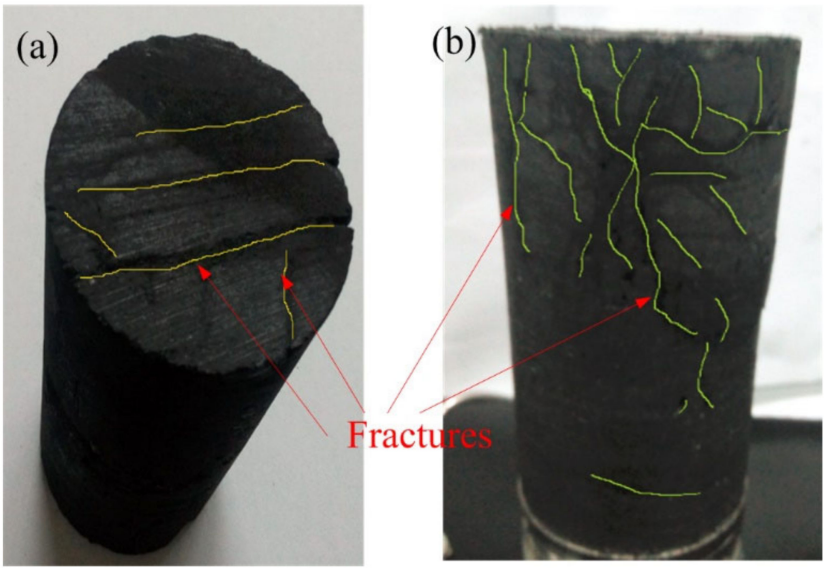

Figure 2. (**a**) A typical naturally fractured coal sample. (**b**) The coal sample after HTN_2 injection.

2.3. Experimental Process

According to the actual situation at the Pingdingshan Coalfield, the geostress pressure is 10 MPa. The experimental conditions of the coal samples are shown in Table 2. The testing process was as follows:

Table 2. Experimental conditions for six specimens.

Coal Sample	N_2 Temperature/°C	N_2 Injection Pressure/MPa	Cycle Number
S-60-4	60	4	1
S-60-6	60	6	1
S-60-8	60	8	1
S-80-4	80	4	1
S-100-4	100	4	1
SU-60-4	60	4	3
SU-80-4	80	4	3
SU-60-6	60	6	3
SU-80-6	80	6	3

(1) Coal sample S-60-4 was placed on the indenter located at the bottom of the testing machine and connected to the HTN_2 pipelines.

(2) The pressure chamber was sealed. After the pressure chamber was filled with oil, the oil was heated to 30 °C by the heating ring. Then, hydrostatic pressure was applied to the coal sample S-60-4 at 3 MPa/min until it reached 10 MPa; the confining pressure and axial pressures were kept constant. The heating controller and pressure-regulating valve were adjusted to ensure that the N_2 temperature was 60 °C and that the N_2 injection pressure was 4 MPa.

(3) The flow rate and gas injection time were recorded during the test. The beginning time was defined as when the flow rate of the outlet was observed and remained constant. When the flow rate at the outlet suddenly increased and remained constant (the change of flow rate was within 5%) for at least 15 min, the N_2 injection was stopped with the temperature and pressure. The test was then completed.

(4) Steps (1), (2) and (3) were repeated with the remaining samples.

Currently, the measurements of the coal sample permeability are mainly via steady-state and transient methods. The flow of N_2 in the coal sample is laminar, and Ranjith et al. used a steady-state method to measure the N_2 permeability of low-permeability coal. Based on this, the steady-state method was chosen to perform this experiment [20]. The HTN_2 permeation through the coal sample is assumed to be an isothermal process, and the ideal gas law is applicable. The N_2 permeability is calculated by [21]:

$$k = \frac{2QP_{out}\mu L}{A(P_{in}^2 - P_{out}^2)} \quad (1)$$

In this paper, the permeability k is defined in SI units of m^2. The conversion factor from m^2 to mD is expressed by 1 mD = 10^{-15} m^2.

3. Results and Discussion

3.1. Permeability Evolution under N_2 Injection

Figure 2b presents the surface fracture growth of sample S-100-4 after the N_2 injection. New fractures were visually observed from the sample surfaces. The evolution of the coal permeability ratio with time is shown in Figures 3 and 4. As seen from the figure, during the N_2 injection process, the permeability ratio decreases over time in the beginning, suddenly increases to a large value, and is then maintained within a relatively stable range. To explain the experimental phenomena, the existing model has been cited and revised. The permeability of a natural fracture depended on the fracture permeability, so the fracture permeability was used to analyze the evolution of the coal permeability [19]. Appendix A presents the effective strain of the fractures and the permeability variation equations for N_2.

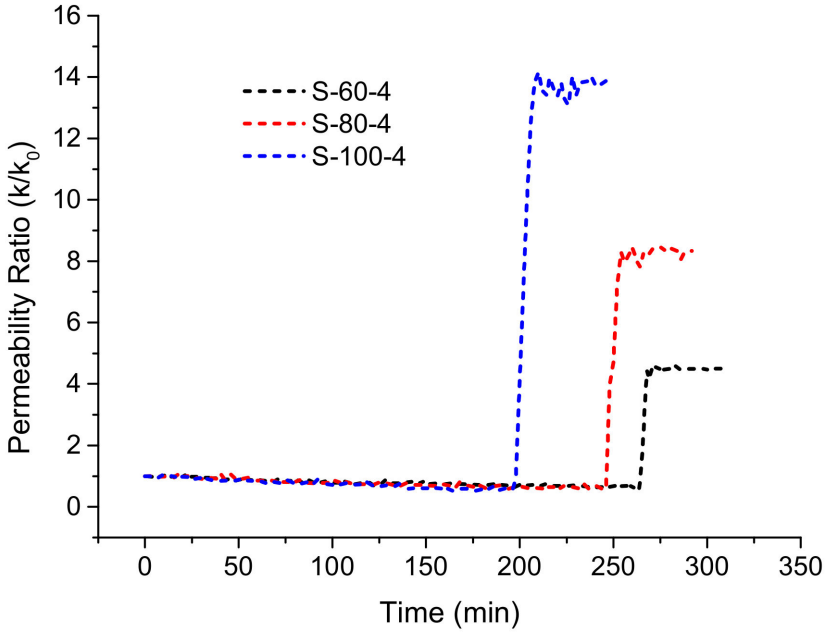

Figure 3. Evolution of the coal permeability ratio with time under different N_2 temperatures.

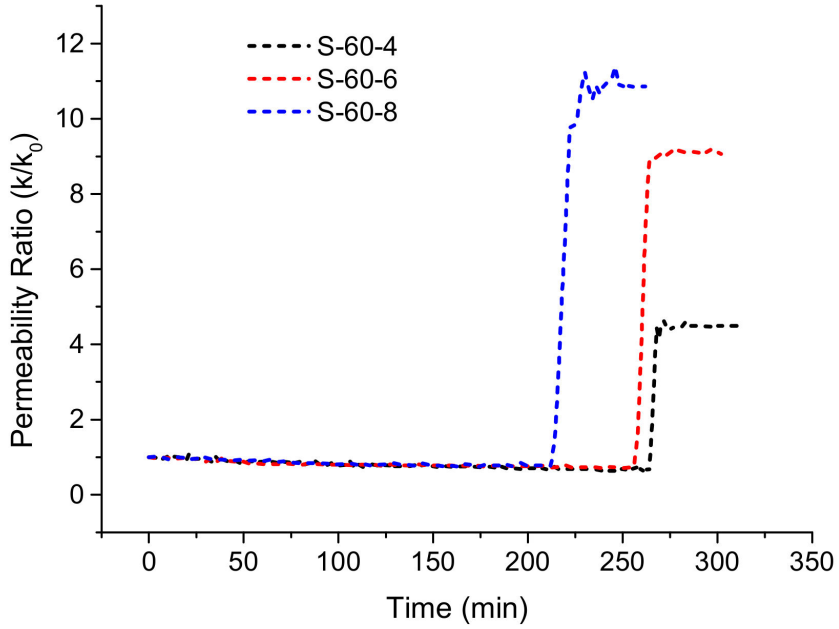

Figure 4. Evolution of the coal permeability ratio with time under different N_2 injection pressures.

When the N_2 injection begins, the matrix pressure is lower than the fracture pressure. Thus, the coal global strain is lower than the fracture local strain [22]. On the fracture surface, the adsorption expansion and thermal expansion occur. According to Equations (A1), (A2) and (A4), the rise of the sorption-induced strain of fracture $\Delta\varepsilon_{fs}$ and the thermal strain of fracture $\Delta\varepsilon_{fT}$ cause the decline of the fracture local strain $\Delta\varepsilon_{fl}$. This decline then leads to the decrease of the effective volumetric strain $\Delta\varepsilon_{fe}$ and the decrease of the fracture permeability k_f, forming a decline phase with a "V" shape.

According to Harpalani and Chen, the coal effective stress subjected to fluid pressure can be calculated using Equation (2) [23]:

$$\sigma_e = p_c - \frac{p_{in} + p_{out}}{2} \tag{2}$$

With a continuous HTN_2 injection, the HTN_2 pressure propagates into the coal matrix, and the matrix pressure rises while the effective stress decreases (Equation (2)). According to Equations (A1), (A3) and (A4), both the thermal expansion of the matrix $\alpha_{mT}(1-\phi_f)T$ and the adsorption-induced expansion of the matrix $(1-\phi_f)\varepsilon_{ms}$ increase, resulting in the increase of the coal global strain ε_v. Thus, the effective volumetric strain $\Delta\varepsilon_{fe}$ and fracture permeability increase, forming an increase phase with a "V" shape. Therefore, the test results of the coal permeability evolution obey the "V" shape.

3.2. Effect of N_2 Temperature on Permeability Evolution

With a continuous HTN_2 injection and under the interaction of HTN_2 and the temperature difference of the coal sample, heat transfer occurs between the coal and HTN_2. The temperature of the coal sample gradually increases. The results revealed that when the coal temperature increased from 30 °C to 70 °C, the triaxial compressive strength of coal was reduced by more than 42%, and the axial strains were reduced by more than 35% [24]. That is to say, the capacity for ductile deformation of coal was weakened with the increase of the temperature.

The higher the N_2 temperature is, the more intense the thermal expansions of the fracture surface and the matrix become. In accordance with Equations (A1), (A2) and (A4), due to the thermal expansion of the fracture surface, the fracture aperture is reduced. The greater permeability attenuation in the initial stage is therefore a result of the higher N_2 temperature. When the N_2 injection pressure is 4 MPa, the permeability attenuation values in the initial stage, which correspond to N_2 temperatures of 60 °C, 80 °C and 100 °C, are 34.3%, 41.3% and 46.9%, respectively (Figure 5). With a continuous N_2 injection, the coal global strain increases. According to Equations (A1), (A3) and (A4), the higher the N_2 temperature, the more intense the integral thermal expansion becomes, which increases the fracture aperture. Thus, the higher the N_2 temperature, the greater the maximum permeability ratio. When the N_2 injection pressure is 4 MPa, the coal maximum permeability ratio values at N_2 temperatures of 60 °C, 80 °C and 100 °C are 4.48, 8.38 and 14.25, respectively (Figure 5).

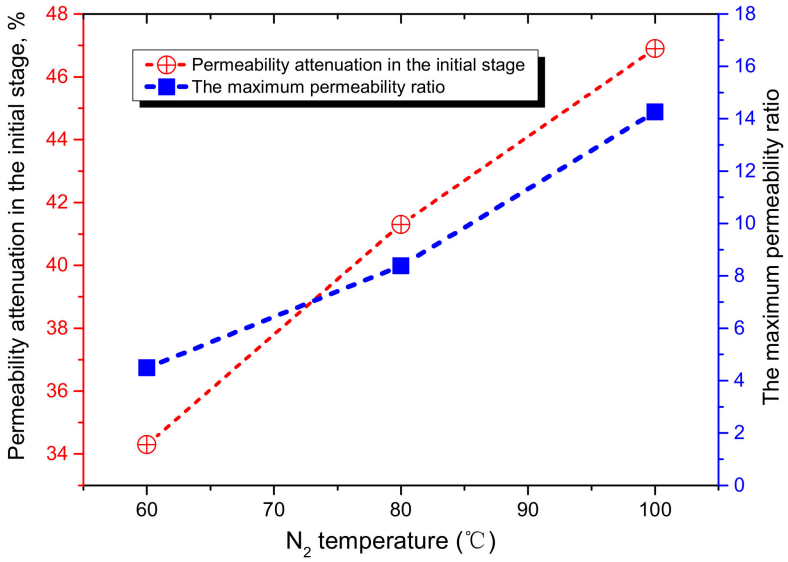

Figure 5. Variation of the permeability attenuation in the initial stage, and the maximum permeability ratio with the N_2 temperature.

3.3. Effect of N_2 Injection Pressure on Permeability Evolution

The greater the N_2 injection pressure is, the greater $\frac{(p_f - p_m)}{K_m}$ and the more intense the compression degree of the matrix in the initial stage will become. p_m is the matrix pressure of coal, p_f is the fracture pressure of coal, and K_m is the bulk modulus of the coal matrix. According to Equations (A1), (A2) and (A4), the smaller the magnitude of the fracture, the smaller the aperture and the permeability attenuation. When the N_2 temperature is 60 °C, the permeability attenuation in the initial stage is 34.3% at a 4 MPa injection pressure, 30.5% at a 6 MPa injection pressure and 25.4% at an 8 MPa injection pressure (Figure 6). The greater the N_2 injection pressure, the greater the fracture pressure and matrix pressure; thus, the effective stress will be smaller, while the adsorption expansion of the fracture surface and the matrix (i.e., ε_{ms} and ε_{fs}) will be larger. According to Equations (A1), (A3) and (A4), the coal global strain increases and the fracture aperture rises, resulting in an increase of the coal permeability. Therefore, the greater the injection pressure, the greater the maximum permeability ratio. When the N_2 temperature is 60 °C, this corresponds to a maximum permeability ratio of 4.48 for a 4 MPa injection pressure, 9.07 for a 6 MPa injection pressure and 10.37 for an 8 MPa injection pressure (Figure 6).

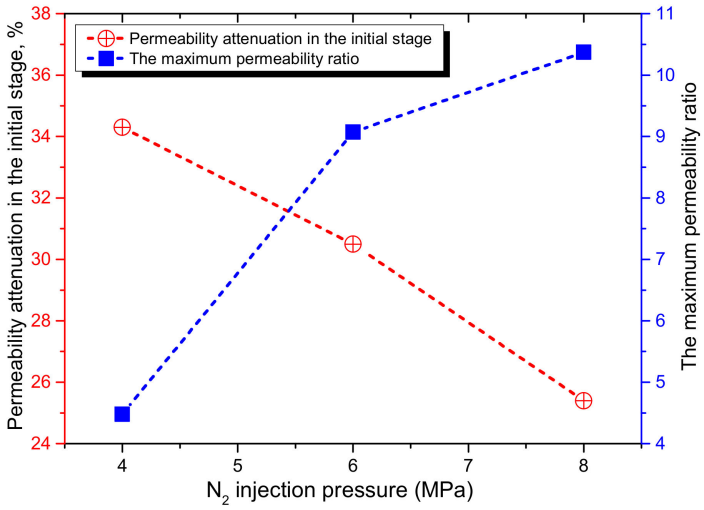

Figure 6. Variation of the permeability attenuation in the initial stage, and the maximum permeability ratio with the N_2 injection pressure.

3.4. Effect of Cycle Number on Permeability Evolution

Figure 7a–d shows the permeability ratio evolution with time under an N_2 injection with three cycles. As seen from the figure, the variation of the coal permeability ratio during various cycles of N_2 injection is the same during the test; they are all in the shape of a V, but the degree of change is constantly reduced. Under the multicycle N_2 injection, the coal sample will be affected by alternating stress. Practice shows that the failures and the static stress caused by the alternating stress are completely different. The alternating stress, the stress that is generated when a fatigue rupture of the coal occurs, is always lower than its static strength. For coal with initial pores and fractures, under the effects of alternating stress, fractures will be further produced and extended, which may well increase the coal permeability.

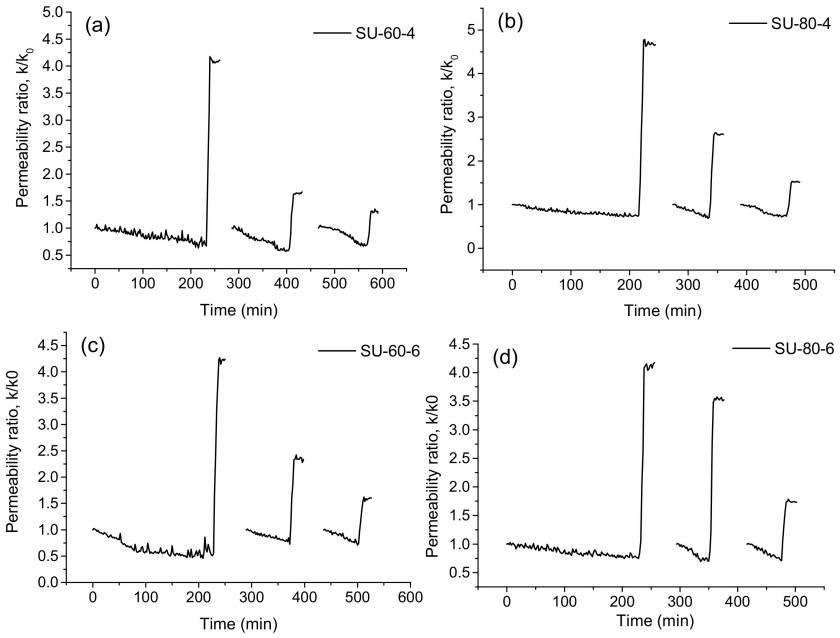

Figure 7. Evolution of the permeability ratio with time under an N_2 injection with three cycles. (**a**) N_2 temperature is 60 °C, and N_2 injection Pressure is 4MPa. (**b**) N_2 temperature is 80 °C, and N_2 injection Pressure is 4MPa. (**c**) N_2 temperature is 80 °C, and N_2 injection Pressure is 6MPa. (**d**) N_2 temperature is 80 °C, and N_2 injection Pressure is 6MPa.

The Paris law, which was proposed by Paris and Erdogan, is used to predict the fracture growth [25]:

$$\frac{da}{dn} = C(\Delta K)^m \tag{3}$$

From this, the growth of the fatigue fractures is related to the maximum and minimum of the alternating stress. In the multicycle N_2 injection process, when alternating the stress amplitude, the coal suffered changes and the expanded degree of fractures could be studied by using the accumulated damage theory.

Palmgren–Miner's rule determines the fatigue strength of coal. When there are f different stress ranges, S_i ($1 \leq i \leq f$) acts on a coal structure, and each S_i contributes n_i cycles. Then, the sum of the fatigue damage is [26]:

$$D = \sum_{i=1}^{f} \frac{n_i}{N_i} \tag{4}$$

During the test, $f = 1$. In other words, the expansion of the coal fracture always occurs when N_2 is injected into the coal sample. According to Palmgren–Miner's rule, the multicycle N_2 injection is propitious to the re-expansion of coal fractures and the increase of coal permeability. The maximum permeability ratio of every period is greater than 1.0. However, based on the original fractures, the re-expansion of the coal volume requires more energy, and thus the mutation degree is declined.

The final permeability ratio of the coal samples S-60-4 and SU-1 was compared. It was observed that the final permeability ratio of sample SU-1 was increased by 101% when compared with sample S-60-4. In other words, the coal permeability increased with the increase of cycle numbers. This is meaningful for the fast gas extraction of low-permeability coal seams. After extracting CBM for a long time, the CBM concentration of boreholes will decrease from 6% to 20%. Such a low CBM concentration can lead to CBM not being usable, which will cause greenhouse effects if CBM is released directly. Therefore, the HTN_2 can be repeatedly injected into the coal seam to realize a CBM extraction with a high CBM concentration and a large flow until the CBM extraction rate meets the national standards.

The permeability of the #J15 coal seam of the Pingdingshan Coalfield in China is 0.0019 md (less than 1 md), the relative gas emission is 123.376 m^3/t, the absolute gas emission is 9.573 m^3/min, the gas pressure is 1.5–2.0 MPa, the gas content is 20–22 m^3/t, and the gas drainage is difficult. In order to make the coal seam meet the requirements of safe mining as soon as possible, the conventional HTN_2 injection method can be used to increase the permeability of coal, followed by gas drainage. When the gas concentration is lower than 20%, HTN_2 can be injected into the coal seam many times, and the permeability of the coal seam can be further increased so as to realize the safe and rapid mining of coal.

4. Conclusions

The effects of the N_2 temperature, injection pressure and cycle number on the permeability of naturally fractured coking coal were investigated. Our main results are as follows:

(1) When HTN_2 was injected into the coal sample, the matrix pressure was lower than the fracture pressure in the beginning, and the coal global strain was lower than the local fracture strain. On the fracture surface, adsorption expansion and thermal expansion occur. Then, the rise of the sorption-induced strain of the fracture and thermal strain of the fracture cause the decline of the fracture local strain, which leads to decreases in the effective volumetric strain and fracture permeability. With a continuous HTN_2 injection, the gas pressure propagates into the matrix, and the matrix pressure rises. Both the thermal expansion and the adsorption expansion of the matrix increase, resulting in the increase of the coal global strain. Thus, the effective volumetric strain and fracture permeability increase. The maximum permeability ratio increases with the rise of the N_2 injecting pressure and temperature.

(2) When multicycle N_2 was injected into the coal sample, the maximum permeability ratios in various cycles were all greater than 1.0 while progressively declining. It is thus clear that alternating stress is conducive to the further expansion of coal fractures and an increasing coal permeability. On the basis of the first period of expansion, re-expansion is difficult and requires more energy. The effects of multicycle N_2 injection on coal permeability has been considerably improved when compared with N_2 injection with only one cycle.

Author Contributions: S.W. conceived and designed the experiments; S.W., H.L. and L.H. performed the experiments; S.W. and L.H. analyzed the data; S.W. and H.L. wrote the paper. All authors have read and agreed to the published version of the manuscript.

Funding: This research was supported by the National Natural Science Foundation of China (No. 51904270).

Institutional Review Board Statement: Not applicable.

Informed Consent Statement: Not applicable.

Data Availability Statement: Data sharing not applicable.

Acknowledgments: The authors thanks Fubao Zhou's team at China University of Mining and Technology for their help.

Conflicts of Interest: The author declares no conflict of interest.

Abbreviations

k	the coal permeability (m^2)
P_{in}	the HTN_2 pressure at the inlet of the sample (Pa)
Q	The HTN_2 permeation rate (m^3/s)
L	the length of the sample (m)
σ_e	the coal effective stress
P_{in}	the inlet pressure
$\Delta\varepsilon_{fe}$	the effective strain of coal fractures
$\Delta\varepsilon_{fl}$	the coal fracture local strain
p_f	the fracture pressure of coal
$\Delta\varepsilon_{fT}$	the thermal strain of coal fracture
K	the coal bulk modulus
α_m	the Biot coefficient of the coal matrix
α_{mT}	the thermal expansion coefficient of the coal matrix
T	the coal temperature
ϕ_f	the current coal fracture porosity
k_f	the current fracture permeability of coal
a	the flaw depth of coal
C	the material constants
N_i	the number of loading cycles to failure under a constant stress range
A	the cross-sectional area of the coal sample (m^2)
P_{out}	the HTN_2 pressure at the outlet of the sample (Pa)
μ	HTN_2 kinematic viscosity (Pa·s)
Pc	the confining pressure
P_{out}	the outlet pressure
$\Delta\varepsilon_{fs}$	gas sorption-induced strain of the coal fracture
$\Delta\varepsilon_v$	The coal global strain
p_m	the matrix pressure of coal
K_m	the bulk modulus of the coal matrix

ε_v	the coal global strain
$\overline{\sigma}$	the coal mean stress
α_f	the Biot coefficient of the coal fracture
α_{fT}	the thermal expansion coefficient of the coal fracture
ε_{ms}	The gas sorption-induced strain of the coal matrix
k_{f0}	the initial fracture permeability of coal
ϕ_{f0}	the initial fracture porosity of coal
$\triangle$K	the stress intensity factor range in a stress cycle
m	the material constants
D	the fatigue damage

Appendix A. Permeability Variation Model

The effective strain of coal fractures is the resultant strain of the coal fracture local strain and the coal global strain [19]. The change of the effective volumetric strain is:

$$\Delta\varepsilon_{fe} = \Delta\varepsilon_v + \Delta\varepsilon_{fl} \tag{A1}$$

In the coal permeability model, the temperature impact has not been taken into account. If the model is revised and the thermal expansion effect of the matrix is taken into consideration, then the fracture local strain is:

$$\Delta\varepsilon_{fl} = \frac{(p_f - p_m)}{K_m} - \Delta\varepsilon_{fs} - \Delta\varepsilon_{fT} \tag{A2}$$

The coal global strain (ε_v) can then be calculated as follows:

$$\varepsilon_v = \frac{1}{K}(\overline{\sigma} + \alpha_m p_m + \alpha_f p_f) + \alpha_{mT}(1-\phi_f)T + \alpha_{fT}\phi_f T + (1-\phi_f)\varepsilon_{ms} + \phi_f\varepsilon_{fs} \tag{A3}$$

The fracture permeability was expressed as [19]:

$$\frac{k_f}{k_{f0}} = \left(1 + \frac{\Delta\varepsilon_{fe}}{\phi_{f0}}\right)^3 \tag{A4}$$

References

1. Yuan, L. Key technique of safe mining in low permeability and methane rich seam group. *Chin. J. Rock Mech. Eng.* **2008**, *27*, 1370–1379.
2. Karacan, C.Ö.; Ruiz, F.A.; Cotè, M.; Phipps, S. Coal mine methane: A review of capture and utilization practices with benefits to mining safety and to greenhouse gas reduction. *Int. J. Coal Geol.* **2011**, *86*, 121–156. [CrossRef]
3. Wang, S.C.; Zhou, F.B.; Kang, J.H.; Wang, X.X.; Li, H.J.; Wang, J.L. A heat transfer model of high-temperature nitrogen injection into amethane drainage borehole. *J. Nat. Gas Sci. Eng.* **2015**, *24*, 449–456. [CrossRef]
4. Zhou, F.D.; Hussain, F.; Cinar, Y. Injecting pure N2 and CO_2 to coal for enhanced coalbed methane: Experimental observations and numerical simulation. *Int. J. Coal Geol.* **2013**, *116–117*, 53–62. [CrossRef]
5. Kiyama, T.; Nishimoto, S.; Fujioka, M.; Xue, Z.; Ishijima, Y.; Pan, Z.; Connell, L. Coal swelling strain and permeability change with injecting liquid/supercritical CO_2 and N2 at tress-constrained conditions. *Int. J. Coal Geol.* **2011**, *85*, 56–64. [CrossRef]
6. Connell, L.D.; Sander, R.; Pan, Z.J.; Camilleri, M.; Heryanto, D. History matching of enhanced coal bed methane laboratory core flood tests. *Int. J. Coal Geol.* **2011**, *87*, 128–138. [CrossRef]
7. Chen, Z.W.; Liu, J.S.; Elsworth, D.; Connell, L.D.; Pan, Z.J. Impact of CO_2 injection and differential deformation on CO_2 injectivity under in-situ stress conditions. *Int. J. Coal Geol.* **2010**, *81*, 97–108. [CrossRef]
8. Saghafi, A.; Faiz, M.; Roberts, D. CO_2 storage and gas diffusivity properties of coals from Sydney Basin, Australia. *Int. J. Coal Geol.* **2007**, *70*, 240–254. [CrossRef]
9. Perera, M.S.A.; Ranjith, P.G.; Choi, S.K.; Bouazza, A.; Kodikara, J.; Airey, D. A review of coal properties pertinent to carbon dioxide sequestration in coal seams: With special reference to Victorian brown coals. *Environ. Earth Sci.* **2011**, *64*, 223–235. [CrossRef]
10. Packham, R.; Connell, L.; Cinar, Y.; Moreby, R. Observations from an enhanced gas recovery field trial for coal mine gas management. *Int. J. Coal Geol.* **2012**, *100*, 82–92. [CrossRef]
11. Pan, J.N.; Hou, Q.L.; Ju, Y.W.; Bai, H.L.; Zhao, Y.Q. Coalbed methane sorption related to coal deformation structures at different temperatures and pressures. *Fuel* **2012**, *102*, 760–765. [CrossRef]

12. Santarosa, C.S.; Crandall, D.; Haljasmaa, I.V.; Hur, T.B.; Fazio, J.J.; Warzinski, R.P.; Heemann, R.; Ketzer, J.M.M.; Romanov, V.N. CO_2 sequestration potential of Charqueadas coal field in Brazil. *Int. J. Coal Geol.* **2013**, *106*, 25–34. [CrossRef]
13. Wang, C.G.; Feng, J.L.; Liu, J.S.; Wei, M.Y.; Wang, C.S.; Gong, B. Direct observation of coal–gas interactions under thermal and mechanical loadings. *Int. J. Coal Geol.* **2014**, *131*, 274–287. [CrossRef]
14. Li, Z.Q.; Xian, X.F.; Long, Q.M. Experiment study of coal permeability under different temperature and stress. *J. China Univ. Min. Technol.* **2009**, *38*, 523–527.
15. Hu, Y.Q.; Zhao, Y.S.; Yang, D.; Kang, Z.Q. Experiment study of effect of temperature on permeability characteristics of lignite. *Chin. J. Rock Mech. Eng.* **2010**, *29*, 1585–1590.
16. Zhao, Y.S.; Qu, F.; Wan, Z.J.; Zhang, Y.; Liang, W.G.; Meng, Q.R. Experimental investigation on correlation between permeability variation and pore structure during coal pyrolysis. *Transp. Porous Media* **2010**, *82*, 401–412.
17. Perera, M.S.A.; Ranjith, P.G.; Choi, S.K.; Airey, D. Investigation of temperature effect on permeability of naturally fractured black coal for carbon dioxide movement: An experimental and numerical study. *Fuel* **2012**, *94*, 596–605. [CrossRef]
18. Zhu, W.C.; Wei, C.H.; Liu, J.S.; Qu, H.Y.; Elsworth, D. A model of coal–gas interaction under variable temperatures. *Int. J. Coal Geol.* **2011**, *86*, 213–221. [CrossRef]
19. Peng, Y.; Liu, J.S.; Wei, M.Y.; Pan, Z.J.; Connell, L. Why coal permeability changes under free swellings: New insights. *Int. J. Coal Geol.* **2014**, *133*, 35–46. [CrossRef]
20. Ranjith, P.G.; Perera, M.S.A. A new triaxial apparatus to study the mechanical and fluid flow aspects of carbon dioxide sequestration in geological formations. *Fuel* **2011**, *90*, 2751–2759. [CrossRef]
21. Wang, S.G.; Elsworth, D.; Liu, J.S. Permeability evolution during progressive deformation of intact coal and implications for instability in underground coal seams. *Int. J. Rock Mech. Min. Sci.* **2013**, *58*, 34–45. [CrossRef]
22. Connell, L.D.; Lu, M.; Pan, Z.J. An analytical coal permeability model for tri-axial strain and stress conditions. *Int. J. Coal Geol.* **2010**, *84*, 103–114. [CrossRef]
23. Harpalani, S.; Chen, G. Influence of gas production induced volumetric strain on permeability of coal. *Geotech. Geol. Eng.* **1997**, *15*, 303–325. [CrossRef]
24. Yin, G.Z.; Jiang, C.B.; Wang, J.G.; Xu, J. Combined Effect of Stress, Pore Pressure and Temperature on Methane Permeability in Anthracite Coal: An Experimental Study. *Transp. Porous Media* **2013**, *100*, 1–16. [CrossRef]
25. Paris, P.C.; Erdogan, F. A critical analysis of crack propagation laws. *J. Basic Eng.* **1963**, *85*, 528–534. [CrossRef]
26. Chen, N.Z.; Wang, G.; Soares, C.G. Palmgren–Miner's rule and fracture mechanics-based inspection planning. *Eng. Fract. Mech.* **2011**, *78*, 3166–3182. [CrossRef]